JOURNAL OF MECHANICS OF CONTINUA AND MATHEMATICAL SCIENCES
www.journalimcms.org

ISSN (Online) : 2454 -7190 Vol.-15, No.-11, November (2020) pp 36-45 ISSN (Print) 0973-8975

HIGH DATA RATE WDM SYSTEMS-BASED GRAPHENE CARRIERS

Saib Thiab Alwan

Department of Materials, College of Engineering, University of Diyala, Diyala, Iraq

Corresponding Author: **Saib Thiab Alwan**

Email: saib_alwan_eng@uodiyala.edu.iq

https://doi.org/10.26782/jmcms.2020.11.00004

(Received: September 21, 2020; Accepted: November 4, 2020)

Abstract

In this paper, carrier's generation-based graphene with applicability for wavelength division multiplexing (WDM) systems has been produced via illumination of graphene by 980 nm. This technique allowed for servicing of a greater number of channels in a WDM system, and the carriers were able to travel in an optical channel with a high data rate. Eight carriers, having a frequency spacing (FS) of 25 GHz and full-width at half-maximum (FWHM) of 500 MHz, were created. These generated carriers were separately modulated with eight optical quadrature phase shift keying (QPSK) signals and subsequently optically multiplexed and transmitted to an optical fiber channel. At the receiver side, the received signal was demultiplexed, and the performance of the system was analyzed by calculating the error vector magnitude and constellation diagram of the entire system. Opti System version 17.1 and Matlab software are used for demonstration of the WDM system and carrier generation.

Keywords : WDM system, Graphene-based carrier, Frequency spacing (FS), Quadrature phase shift keying (QPSK), Error vector magnitude (EVM), Eye diagram

I. Introduction

Over the past few years, broadband access providers have faced sustained demands for higher data rates due to a great variety of new bandwidth-hungry services and an accumulating number of end users [II-V]. Preliminary experimental attempts for designing and evaluating an advanced dense wavelength division multiplexing (WDM) system capable of simultaneously transmitting multiple RF signals carrying various broadband wireless services, including ISDB-T signals, cellular phone, wireless LAN, terrestrial digital broadcasting, and upcoming wireless services, [V–XI] since they are more resilient to channel dispersion when compared to conventional time-division multiplexing techniques [XIII, VII]. Moreover, WDM engenders many advantages, such as immunity to chromatic dispersion (CD) and polarization mode dispersion (PMD) in radio-over-fiber transmission systems [XIV–XIX]. One possible solution to increase the number of wavelength division multiplexer (WDM) services is to generate more optical carriers in the transmitter section namely comb source generation. Multicarrier optical sources with narrow channel spacing have emerged to meet demands from networks with dense wavelength-division-multiplexing (WDM) and super dense WDM. Many solutions have been proposed to achieve low-cost compact multicarrier optical sources that would provide all the channels required by optical communication standards. These schemes are based on supercontinuum (SC) generation [X], nonlinear spectral broadening of intensity modulated signals [III, IX]. Dense wavelength division multiplexing (DWDM) is the uncontested candidate for increasing the capacity throughput of optical networks. Optical multiplexers/demultiplexers based on arrayed waveguide gratings (AWGs) are the key components in such DWDM systems because of their low insertion loss, high stability, and low cost [XXI, XXII]. Generally, the generation of microwave signals from optical sources has long been a substantial area of interest due to its large potential for a variety of applications in communications [XXIII]. This is attributed to the optical sampling window, which is sized using electro-absorption modulators (EAMs) and is significantly shorter than its electrical counterpart [XXIII- XV]. Wavelength division multiplexing (WDM) is a technology of multiplex optical wave over one optical link; hence the capacity of transmission data rate can be boosted. In this paper, a simulation of optical WDM communication system has been designed for transmitting 400 Gbps along with maximum ranges of optical fiber using graphene as a multicarrier source.

II. Generating of Carriers-Based Graphene

The description of carrier's generation, in terms of a pulse spectrum that evolves with time, can be transformed into a description of a pulse with a temporal envelope that evolves on a time scale much longer than the pulse width. In the time domain, the laser output consists of a continuous train of pulses, equally spaced by the cavity roundtrip time T_r. This can be described by a convolution with a delta comb function as expressed in Equation 1 [XXIV]:

$$E(t) = A(t).\exp(i\omega_c t) \otimes \sum_{m=-\infty}^{\infty} \delta(t - mT_r) \tag{1}$$

The Fourier-transform of Equation 1 yields a Delta series of optical frequencies which are equally spaced by the pulse repetition rate $f_r = 1/T_r$. For this reason, the output of an illumination of graphene by 980 nm is referred to as an optical carrier as given in Equation 2 [XXIV]:

$$\tilde{E}(f) = \tilde{A}(f) \sum_{m=-\infty}^{\infty} \delta(f - mf_r - f_o) \tag{2}$$

The proposed graphene source for carrier's generation is schematically presented in Fig.1. Overall, the presented system it consists of a ring cavity mode-locked Erbium-doped fiber laser (EDFL), which was designed based on the graphene-SA. The EDFL used 980 nm laser diode (LD) to pump the gain medium via a 980/1550 wavelength division multiplexer (WDM). The gain medium of the laser was a 2 m long of Erbium-doped fiber (EDF) with Erbium ions absorption of 23 dB/m at 980 nm. The EDF has a numerical aperture (NA), group velocity dispersion (GVD), and the core and cladding diameters of 0.16, 27.6 ps2/km, 4 µm, 125 µm, respectively. The unidirectionality of the light inside the optical resonator is ensured by using a polarization insensitive isolator (ISO) which is connected to the gain medium directly. This unidirectionality of the light is essential to decrease the probability of damage to the SA or LD that could be caused by the back reflection.

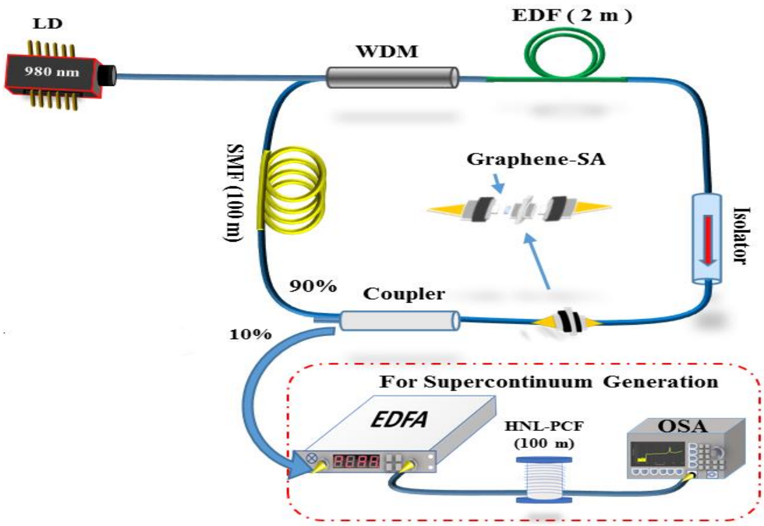

Fig.1 Schematic diagram of the carrier's source-based graphene

III. WDM System-Based Graphene carriers

The transmitter subsystem consists of a carrier source, optical de-multiplexer (De-Mux), optical QPSK modulators and an optical multiplexer (Mux), as displayed in Fig.2. The carrier source part utilized in Section II. The generated carriers by a carrier source are split by the optical demultiplexer and simultaneously applied to external optical modulators (i.e., QPsk). The WDM communication system was designed by Opti System v17.1, which is shown in Fig. 2 and with its parameters of Table (1). This design has eight transmit and receive channels, with each carrying 25 Gbps of data rate placed on the RF signal by a QPSK modulator; the QPSK output optical modulation signal has a change in phase of a carrier wave and constant amplitude. This modulator consists of M-ray so it also called QPSK. The modulation optical signal could transmit through optical channel by employing optical wave when optically modulated by QPSK.

Table **1:** Parameters for the simulated WDM system

Parameter	**Value**
Modulation format	QPsk
Transmission power	10 dBm
Number of channels	8
Frequency spacing	25 GHz
RF signal frequency	25 GHz
Gain of optical amplifier	20 dBm

This design consists of eight QPSK to send eight optical modulation signals; these signals combined together to produce an optical signal transporting over the optical medium. Hence, carriers have been employed by WDM system to transport 400 Gbps of information over single mode optical fiber; WDM communication for enhancement of the system performance by transporting more than one signal at the same time, due to optical channel ability of high immunity RF signals interference. However, the wavelength division de-multiplexing (De-WDM) separated and distributed the wavelengths at receiver, and the receiver section consists PD photodiodes, OBPF to extract the transmitted RF, and QPsk demodulator (demod.) for extracting input data. The transmission link utilizes N_{span} identical spans. Each fiber span consists of a standard single-mode fiber (SMF), a dispersion compensating fiber (DCF), and an optical amplifier (OA). A full periodic dispersion map is adapted to compensate for the dispersion by employing a DCF after the SMF (i.e., post-compensation). For compensating the fibers losses, OAs are employed. The WDM receiver comprises an optical band-pass filter (OBPF), and optical PSK demodulators. Optical de-multiplexers are directly employed to split and filter the subcarriers. After that, the resulting signals were sampled by MZMs. Afterward, the output from each MZM is filtered by the optical band-pass filter and then detected by using optical PSK demodulator.

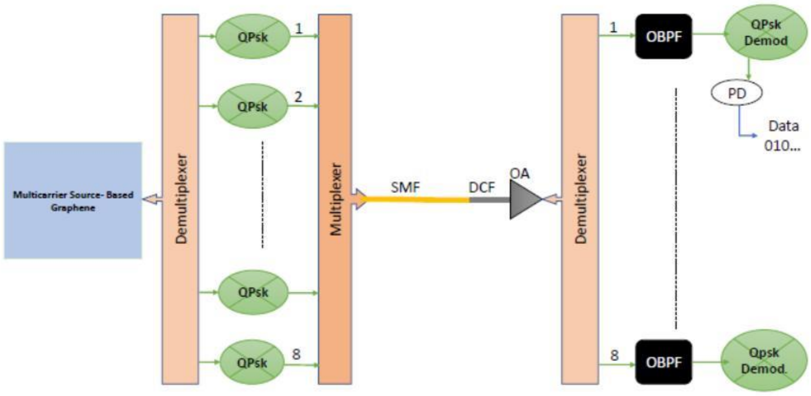

Fig. 2 Schematic diagram of WDM System-Based Graphene Source

IV. Simulation Results and Discussion

The proposed optical WDM system is simulated using OptiSystem commercial software, the numerical simulation results of investigation performance of the WDM system are demonstrated. Moreover, the constellations and eye diagrams for QPSK format were examined with the varying fiber length of the system. The WDM system performance was investigated using QPSK modulation format for eight carriers. At the transmitter side, the optical carrier source provided eight carriers with the frequency spacing of 25 GHz. After splitting the carriers using optical demultiplexer. These carriers were modulated independently using optical QPSK modulators, as. Each separated carrier was modulated at a symbol rate equal to $25\,\mathrm{Gsymbol/s}$, that corresponds to the frequency spacing of the carriers. In this point, the total data rate is equal to $2 \times 8 \times 25\,\mathrm{Gsymbol/s} = 400\,\mathrm{Gbit/s}$. The modulation symbols for each separated carrier was generated by two independent pseudo-random binary sequence (PRBS) signals, each has a length of $(2^{11} - 1)$ bits using a QPSK . Each separated carrier is split by a 3dB coupler and launched into two parallel arms. The in-phase component of the intricate envelope modulates the separated carriers within the upper arm, whereas the quadrature-phase component modulates the 90° shifted separated carrier in the lower arm, and they are combined by another 3dB coupler. Next, all modulated carriers (i.e., QPSK signals) are recombined by the optical multiplexer, yielding an aggregated WDM output signals, as depicted in Fig. 3.

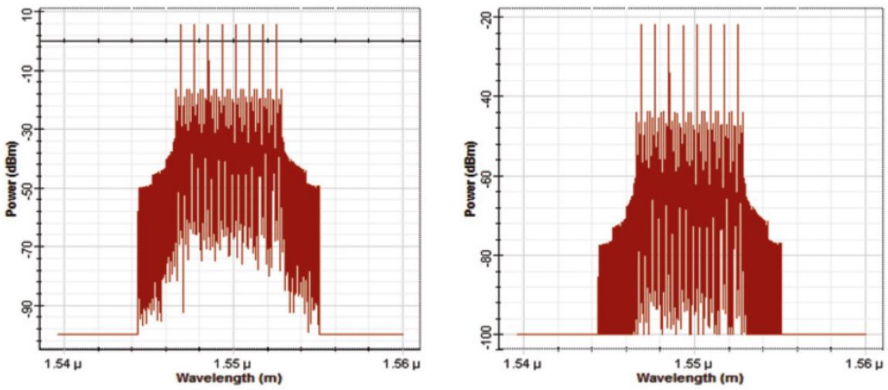

(a) (b)

Fig**.3** Optical spectra of obtained WDM signals a) at the transmitter side (b) at the output of 1500 km optical fiber.

For performance measurement of the WDM system, constellation diagrams and the corresponding eye diagrams are illustrated in Figs. 4 and 5, respectively. The constellation diagram describes the signal that digitally modulated, presenting it as a two-dimensional dispersion diagram. Figs. 4 and 5 display the constellation diagrams and the corresponding eye diagrams of the QPSK WDM signal at transmission distances of 55 km, 110 km (2 spans), 220 km (4 spans), and 440 km (8 spans). These diagrams were obtained for 193.1 THz channel at the output of the QPSK receiver. Furthermore, these simulation results are obtained at each transmission distance. Where the ideal constellation is plotted by a blue sphere. Fig. 4, it is shown that the WDM employed eight carriers produces clearer constellation diagrams. In addition as the transmission distance increases the constellation is squeezed for both comb lines numbers.

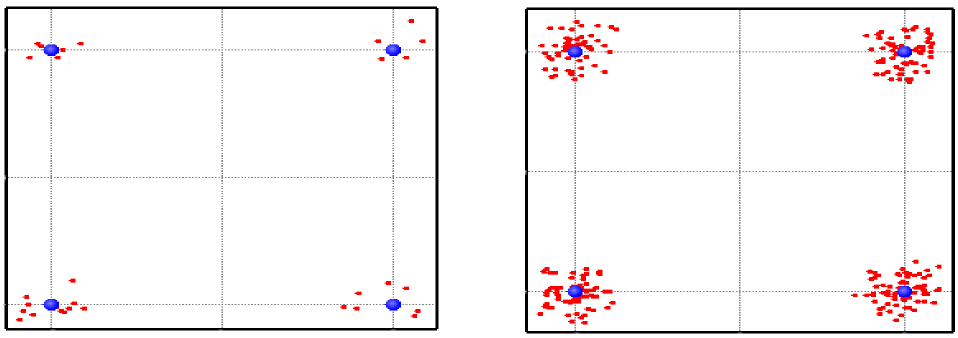

(a) (b)

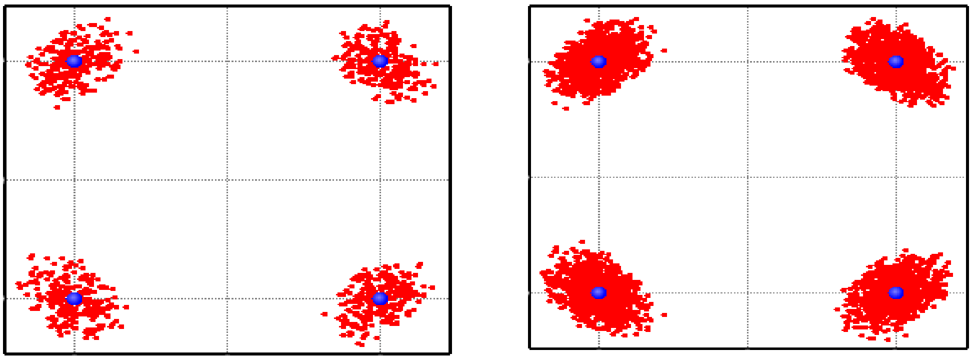

(c) **(d)**

Fig.4 Received constellation diagrams after transmission over (a) 55 km, (b) 110 km, (c) 220 km, and (d) 440 km.

It is clear from Fig. 5 that, the eye diagrams for WDM employed eight carriers. Moreover, the eye openings slowly close with increasing the transmission distance. From Fig. 5, this degradation of signal due to increasing the noise and the fiber nonlinearities. The difference in timing and amplitude from bit to bit cause the eye-opening to shrink. For Fig. 5, there is an open eye for each case that shows a possible successful reception.

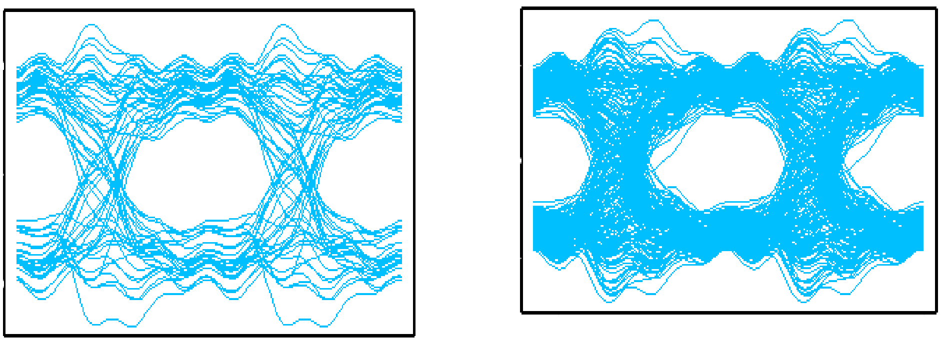

(a) (b)

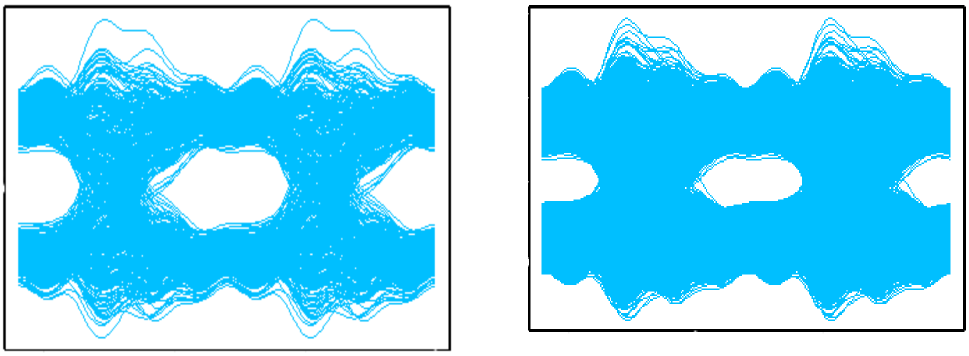

(c) (d)

Fig. 5 Eye diagrams after transmission over (a) 55 km, (b) 110 km, (c) 220 km, and (d) 440 km

V. Conclusion

The basic aim of this paper is to design and investigate the performance of optical WDM system using graphene as a carrier source, each generated carrier has been modulated by an optical quadrature PSK format with a symbol rate of 25 Gsymbol/s. Moreover, the production technique provided for greater number of channels for servicing in an optical WDM system have been quantitatively explored. The total capacity of the system increases as the number of carriers increases. However, system performance is degraded. Data rates of 400 Gbit/s can be achieved at the threshold bit error rate of BER $= 1 \times 10^{-3}$ over a transmission distance of 3000 km using eight carriers.

Conflict of Interest:

There is no conflict of interest regarding this article

References

I. Amulya Boyina, Praveen Kumar Kancherla, : Active Coplanar Wave guide Fed Switchable Multimode Antenna Design and Analysis, J. Mech. Cont.& Math. Sci., Vol.-14, No.-4, July-August (2019) pp 188-196.

II. A. Bekkali, C. Ben Naila, K. Kazaura, K. Wakamori, and M. Matsumoto, “Transmission analysis of OFDM-based wireless services over turbulent radio-on-FSO links modeled by Gamma-Gamma distribution,” IEEE Photonics J., vol. 2, no. 3, pp. 510–520, Jun. 2010.

III. A. Hammoodi, L. Audah, and M. A. Taher, "Green Coexistence for 5G Waveform Candidates: A Review," IEEE Access, vol. 7, pp. 10103-10126, 2019

IV. A. Hraghi, M. E. Chaibi, M. Menif, and D. Erasme, "Demonstration of 16QAM-OFDM UDWDM transmission using a tunable optical flat comb source," journal of lightwave technology, vol. 35, pp. 238-245, 2016

V. A. M. Jaradat, J. M. Hamamreh, and H. Arslan, "Modulation Options for OFDM-Based Waveforms: Classification, Comparison, and Future Directions," IEEE Access, vol. 7, pp. 17263-17278, 2019

VI. A. Mostafa and S. Hranilovic, "In-field demonstration of OFDM-over-FSO," IEEE Photon. Technol. Lett., vol. 24, no. 8, pp. 709–711, Apr. 2012.

VII. Al Naboulsi M, Sizun H, De Fornal F. Fog attenuation prediction for optical and infrared waves. Opt Eng. 2004;43(2):319‑29.

VIII. Amphawan A, Chaudhary S, Chan V. 2 × 20 Gbps-40 GHz OFDM Ro-FSO transmission with mode division multiplexing. J Eur Opt Soc-Rapid Public. 2014;9:14041.

IX. Amphawan A, Chaudhary S, Chan VWS. 2 × 20 Gbps-40 GHz OFDM Ro-FSO transmission with mode division multiplexer. Europ Opt Soc Rap Public. 2014;9:14041.

X. C. B. Naila, K. Wakamori, M. Matsumoto, A. Bekkali, and K. Tsukamoto, "Transmission analysis of digital TV signals over a radio-on-FSO channel," IEEE Commun. Mag., vol. 50, no. 8, pp. 137–144, Aug. 2012.

XI. Chaudhary S, Amphawn A. 4 × 2.5Gbps=10Gbps RO-FSO transmission system by incorporating hybrid WDM-MDM of spiral phased LG-HG Modes. International Conference on internet applications, protocols and services, 978-967-0910-06-2. 2015.

XII. CH. S. N. Sirisha Devi, B. Vijayakumar, Sudipta Ghosh, : CACHING AND NETWORK RELATED SOLUTIONS FOR: 4G TO 5G TECHNOLOGY IN WIRELESS COMMUNICATIONS, J.Mech.Cont.& Math. Sci., Vol.-14, No.2, March-April (2019) pp 402-426

XIII. E. Wong, "Next-generation broadband access networks and technologies," J. Lightwave Technol., vol. 30, no. 4, pp. 597–608, Feb. 2012.

XIV. Foschini GJ. Layered space-time architecture for wireless communication in a fading environment when using multi-element antennas. Bell Labs Tech J. 1996;1:41‑59.

XV. Gupta MS. What is RF? Microwave Magazine, IEEE. 2002 August 6;12:16.10.

XVI. Haykin S. Communication system, 4th, 2000. "Pass Band Data Transmissions", McMaster University, John Wiley & Sons, Inc., "PassBand Data Transmissions", chapter 6, ISBN 0-471-17869-1.

XVII. K. Kazaura et al., "RoFSO: A universal platform for convergence of fiber and free-space optical communication networks," IEEE Commun. Mag., vol. 48, no. 2, pp. 130–137, Feb. 2010.

XVIII. K. Mori, H. Takara, and S. Kawanishi, "Analysis and design of supercontinuum pulse generation in a single-mode optical fiber," J. Opt. Soc. Amer. B, vol. 18, no. 12, pp. 1780–1792, 2001

XIX. M. Matsumoto et al., "Experimental investigation on a radio-on-free-space optical system suitable for provision of ubiquitous wireless services," PIERS Online, vol. 6, no. 5, pp. 400–405, 2010.

XX. M. S. Chowdhury, M. Kavehrad, W. Zhang, and P. Deng, "Combined CATV and very-high-speed data transmission over a 1550-nm wavelength indoor optical wireless link," in Proc. SPIE OPTO, 2014, Art ID. 901009.

XXI. N. Madamopoulos et al., "Applications of large-scale optical 3D-MEMS switches in fiber-based broadband-access networks," Photon. Netw. Commun., vol. 19, no. 1, pp. 62–73, Feb. 2010.

XXII. Polla DL, Wolfson MB, "RF MEMS integration present & futuretrends", Radio-Frequency Integration Technology, RFIT, 2009.

XXIII. Refa HH, SIuss JJ, Jr., Refai HH, "The transmission of multiple RF signals in free-space optics using wavelength division multiplexing" Proceedings of SPIE Vol 0.5793, 2005.

XXIV. S. E. Alavi et al., "W-band OFDM for radio-over-fibre direct-detection link enabled by frequency nonupling optical upconversion," IEEE Photon. J., vol. 6, no. 6, Dec. 2014, Art ID. 7903908.

XXV. Wake D, Nkansh A, Gomes NJ, Senior Member IEEE. Radio over fiber link design for next generation wireless systems. J Light Wave Technol. 2010;28(16):2456-64.